3D Object Reconstruction Using Single Image

M.A. Mohamed[1], A.I. Fawzy[1] E.A. Othman[2]

[1] Faculty of Engineering-Mansoura University-Egypt

[2] Delta Academy of Science for Engineering and Technology-Egypt

Abstract

Recentely, many algorithms were implemeneted; in order to get better and accurate 3D modeling. In this paper, five proposed methods were presented for 3D object reconstruction from a single 2D color image. The basic idea of the five proposed algorithms: depend on changing the process of 3D reconstruction from single image to 3D reconstruction using two images on which feature extraction and matching were applied and after finding correspondences a 3D model can be obtained. Kanade-Lucas-Tomasi (KLT) and Scale Invariant Feature Transform (SIFT) algorithms used for feature extraction and matching. Experiments were applied in this approach to explore the effectiveness of our methods.

Keywords: *Kanade-Lucas-Tomasi (KLT), Scale Invariant Feature Transform (SIFT).*

1. Introduction

Today there is more and more demand to obtain high accuracy 3D information from 2D images. Increasing demand of requiring 3D models for several applications has resulted in major developments, especially in the case where camera parameters are unknown. Major developments has been done in the case of uncalibrated reconstruction where the camera internal information is unknown. Uncalibrated reconstruction is a more generic case, where images taken by any hand-held camera are used for structure computation [1]. 3D reconstruction is needed in many different areas such as creating movies and animations. In industry very accurate models are used for physical simulations or quality tests. In addition computer games or visualizations are going to be more and more photo-realistic, so the models have to look like real objects which is easy and quickly done with a good reconstruction tool. 3D reconstruction from images is also widely applied in the medical industry. It has been used to create models of a whole range of organs, as well as brains and even teeth. Other application areas include body motion modeling, teleconferencing, robot navigation, object recognition, surveillance, and surveying such as the modeling of terrain and buildings [2].

2. Related Work

3D reconstruction from only one image is a challenging problem in computer vision. From the eighties of the last century more and more algorithms showed up for 3D reconstruction from a single still image. Peter Kovesi [3] reconstructed the shape of the object from its surface normal so called shapelets, which was very simple to implement and robust to noise. Delage, Lee, and Ng [4] built the 3D model of indoor scenes which only contains the vertical walls and ground from single image based on the model using the dynamic Bayesian network. Torralba and Oliva [5] worked on Fourier Spectrum of the image and with it they compute the mean depth of the image. Felzenszwalb and Huttenlocher [6] developed a method for the image segmentation based on the content of the image. It was the first time; where the superpixel was defined which nowadays becomes a foundation for the many algorithms to reconstruct the 3D structure. Most information are available when one has multiple views of the scene, but when only one view is available, additional assumptions must be imposed on the scene [7-11]. Barron and Malik [12] reconstruct albedo; depth; normal, and illumination information from grayscale and color images by inferring statistical priors.

The work in this paper follows most closely from [13], which depends on the concept that humans feel the 3D subjects with two eyes; it is easy to get the information of everything. But with only one eye, it will be hard and even impossible to perceive the depth and other 3D information of the image. So they tried to create a new image from the original one. The new image is created by shifting every pixel of the original image only in the horizontal direction. With the two images, people can easily build the 3d structure based on the human's psychology and physiological function. To reconstruct a 3D model from two images, we depend on the method proposed in [14], in which features were extracted from the two images. The extracted features were then matched across images and after finding correspondences, the 3D model was reconstructed.

Fig. 1 shows the overall structure of the method of 3D reconstruction using horizontal shift.

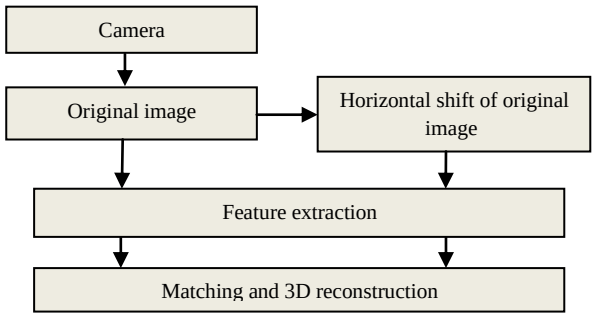

Fig. 1: 3D reconstruction Using Horizontal Shift.

As shown in fig. 1, a camera is used to capture an image of an object and after getting the second virtual image by making horizontal shift for every pixel of the original image, features were extracted from the two images. The extracted features were then matched across images and after finding correspondences, the 3D model was reconstructed.
The remaining of this paper is organized as follows; section-3 introduces Performance Metrics, section-4, provides the proposed methods, section-5 provides experimental results, and section-6 presents conclusion.

3. Performance Metrics

Measurement of the quality of image is important for image processing applications. In general, measurement of image quality usually can be classified into two categories, which are subjective and objective quality measurements. Subjective quality measurement, Mean Opinion Score (MOS), is truly definitive but too inconvenient, the most time taken and expensive. Therefore, objective measurements are developed such as MSE, MAE, PSNR, SC, MD, LMSE, and NAE that are least time taken than MOS but they do not correlation well with MOS [15]. For all the presented methods in this work, MSE, PSNR and NAE were used to compare between the resulted 3D models and the original image in each case. In our analysis, M and N represent number of pixels in row and column directions, respectively. Samples of original image are denoted by x(m,n), while x'(m,n) denotes samples of the resulted 3D model.

2.1 Mean Square Error (MSE)

The simplest of image quality measurement is Mean Square Error (MSE). The large value of MSE means that image is poor quality [15]. MSE can be calculated as follow;

$$MSE = 1/MN \sum_{m=1}^{M} \sum_{n=1}^{N} (x(m,n) - x`(m,n))^2 \quad (1)$$

2.2 Peak Signal-to-Noise Ratio (PSNR)

The small value of Peak Signal to Noise Ratio (PSNR) means that image is poor quality [15]. PSNR is defined as follow:

$$PSNR = 10Log\, 255^2 / MSE \quad (2)$$

2.3 Normalized Absolute Error (NAE)

The large value of Normalized Absolute Error (NAE) means that image is poor quality [15]. NAE is defined as follow:

$$NAE = \sum_{m=1}^{M} \sum_{n=1}^{N} |x(m,n) - x`(m,n)| / \sum_{m=1}^{M} \sum_{n=1}^{N} |x(m,n)| \quad (3)$$

4. Proposed Methods

In this paper, five proposed methods will be introduced.
Fig. 2 shows the overall structure of the first proposed method, in which we used a camera to take an image of an object. Then, a rotation of this image was made by a specified angle. After that features were extracted from the image and the rotated form of it. The extracted features from the two images were matched and after finding correspondences, a 3D model of the object could be reconstructed.

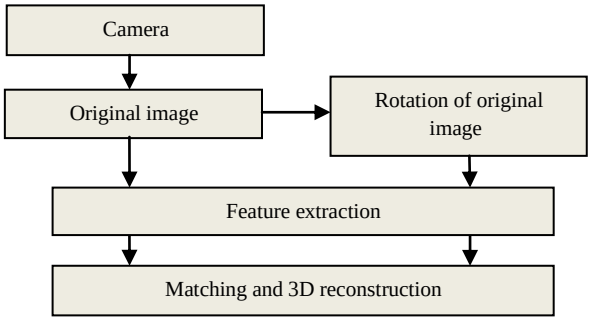

Fig. 2: Overall structure of the first proposed method.

Fig. 3 shows the overall structure of the second proposed method, in which we used only one image to reconstruct two 3D models. Features were extracted from the original image two times. The extracted features were then matched and after finding correspondences, the first 3D model "model1" was reconstructed. This process was repeated between "model1" and the original image to reconstruct "model2".

Fig. 4 shows the overall structure of the third proposed method, in which we used a camera to take an image of an object. Then, a rotation of this image was made by four angles (30, 45, 60, and 90) degree. After that, we used the original image and the four rotated images to reconstruct four 3D models. Local features from the first two images "original image" and "rotated image by 30 degree" were

extracted. The extracted features from two images were then matched and after finding correspondences, the first 3D model "model1" was reconstructed. This process was repeated between "model1" and "rotated image by 45 degree" to reconstruct "model2". "model3" was reconstructed after finding correspondences between the features extracted from "model2" and "rotated image by 60 degree". "model3" and "rotated image by 90 degree" were used to reconstruct "model4".

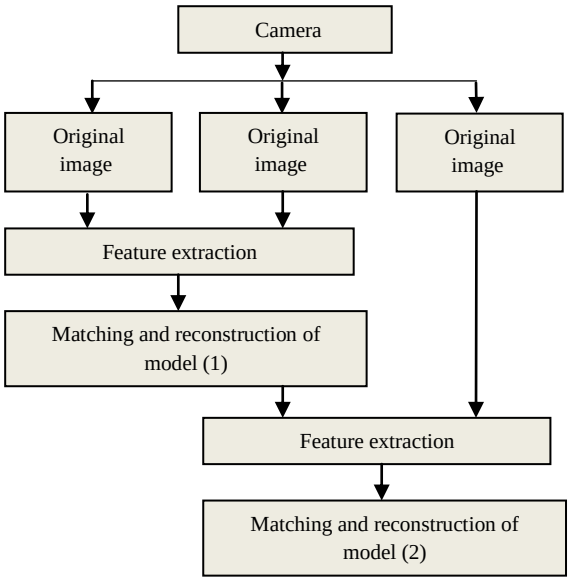

Fig. 3: Overall structure of the second proposed method.

Fig. 5 shows the overall structure of the fourth proposed method, in which a second virtual image was created from an original image. The virtual image was generated by shifting every pixel of the original image in the vertical direction. Features were extracted from the two images. The extracted features were then matched across images and after finding correspondences, the 3D model was reconstructed.

Fig. 6 shows the overall structure of the fifth proposed method, in which a second virtual image is created from an original image. The virtual image was generated by shifting every pixel of the original image in the horizontal direction and shifted the resulted image in the vertical direction. Features were extracted from the two images. The extracted features were then matched across images and after finding correspondences, the 3D model was reconstructed.

For feature extraction and matching, Kanade-Lucas-Tomasi (KLT) and Scale Invariant Feature Transform (SIFT) algorithms were used.

4.1 Overview on SIFT

The SIFT operator is one of the most frequently used operators in the region detector/descriptor panorama. It was first thought up by Lowe [16], and it is currently employed in different computer vision and photogrammetric applications. SIFT is an algorithm widely used in detecting and describing local features in images. Up till today, it remains as one of the most popular feature matching algorithms in the description and matching of 2D image features. The main reason for SIFT to be a successful algorithm in field of feature matching is because it can extract stable feature points. Besides that, it is proven that SIFT is more robust compared to other feature matching techniques as a local invariant detector and descriptor with respect to geometrical changes. It is said to be robust against occlusions and scale variance simple because SIFT feature descriptor is invariant to image translation, scale changes and rotation while partially invariant to illumination changes. Hence, SIFT feature points are used to calculate the fundamental matrix and reconstruct 3D objects. Basically there are four major components in SIFT framework for keypoint detection and extraction [17] as follows;

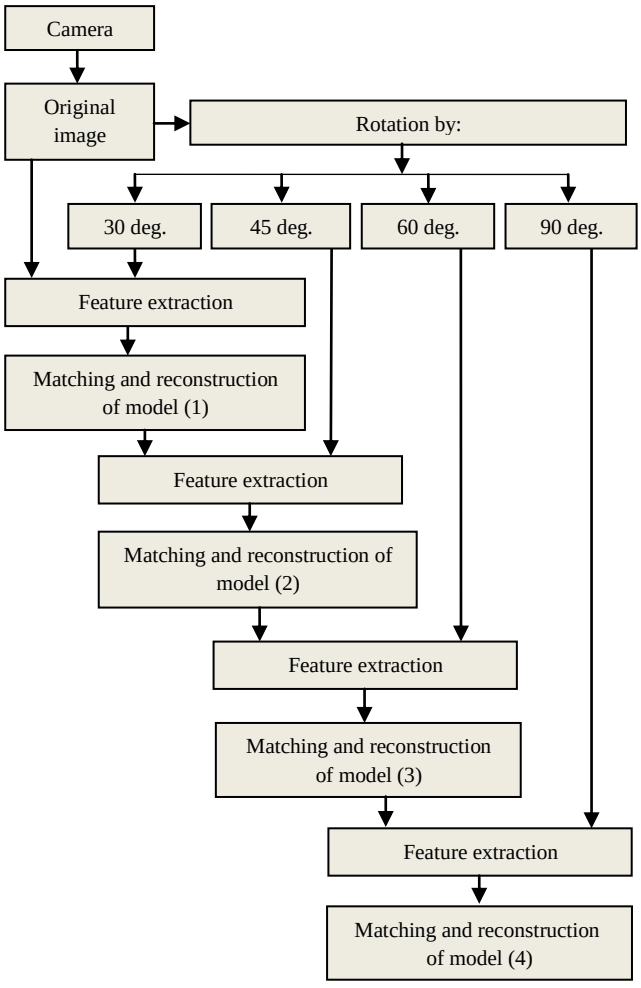

Fig. 4: Overall structure of the third proposed method.

4.1.1 Scale space extreme detection

This is the first stage of computation that searches all scales and image locations. Difference of Gaussian (DOG) function is implemented to detect local maxima and minima. These form a set of candidate keypoints.

4.1.2 Keypoint localization

Every candidate keypoint is fitted to a detailed model for location and scale determination. Low contrast points and poorly localized edge responses are discarded.

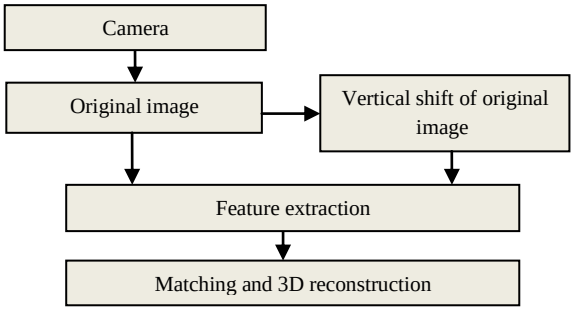

Fig. 5: Overall structure of the fourth proposed method.

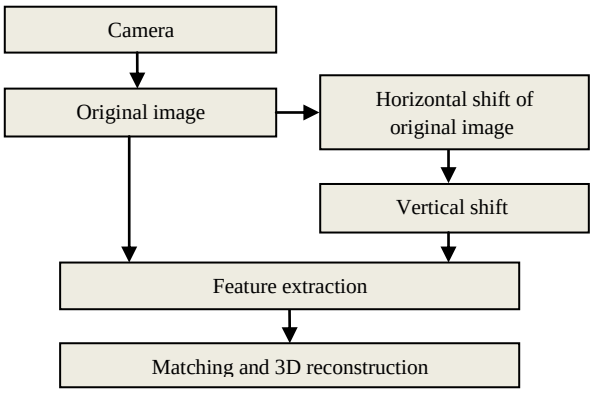

Fig. 6: Overall structure of the fifth proposed method.

4.1.3 Orientation assignment

Based on local image gradient direction, one or more orientations are assigned to each keypoint location.

4.1.4 Keypoint descriptor

The local image gradients are measured at the selected scale in the region around each keypoint.

4.2 KLT overview

In computer vision, the Kanade–Lucas–Tomasi (KLT) feature tracker is an approach to feature extraction. KLT makes use of spatial intensity information to direct the search for the position that yields the best match. It is faster than traditional techniques for examining far fewer potential matches between the images. It locates good features by examining the minimum eigenvalue of each 2 by 2-gradient matrix and uses a Newton Raphson method to track the features by minimizing the difference between the two image windows [18]. To select one the four algorithms for feature extraction, we compare between them using neural network.

5. Experimental Results

In this section, the results of all presented methods will be discussed. In addition, these results will be compared to each other. The performance of all presented methods were tested using three images of RGB type of resolution 1728×2592×3; Fig. 7. Figures (8, 9, and 10) show some cases applied on the three images.

5.1 3D Reconstruction Using Horizontal Shift

A horizontal shift by (0.05, 0.1, and 0.2) % was applied on the three test images according to the method shown in Fig. 1. Table. 1, shows the comparison between the resulted 3D models using SIFT and KLT algorithms with image (1) using Performance Metrics (P.M).

Table 1: Comparison between the resulted 3D models according to 3D Reconstruction Using Horizontal Shift with image (1)

P.M	Shift by 0.05%		Shift by 0.1%		Shift by 0.2%	
	SIFT	KLT	SIFT	KLT	SIFT	KLT
MSE	4.12e+03	4.17e+03	4.27e+03	4.26e+03	4.39e+03	4.41e+03
PSNR	11.98	11.93	11.82	11.84	11.7	11.68
NAE	0.36	0.36	0.38	0.38	0.42	0.42

From the results seen in table 1, we can notice that, the best 3D model was achieved at horizontal shift by 0.05% using SIFT algorithm. Table 2, shows the comparison between the resulted 3D models using SIFT and KLT algorithms with image (2) using Performance Metrics (P.M).

Table 2: Comparison between the resulted 3D models according to 3D Reconstruction Using Horizontal Shift with image (2)

P.M	Shift by 0.05%		Shift by 0.1%		Shift by 0.2%	
	SIFT	KLT	SIFT	KLT	SIFT	KLT
MSE	4.15e+03	4.12e+03	4.18e+03	4.18e+03	4.33e+03	4.33e+03
PSNR	11.95	11.98	11.92	11.92	11.77	11.77
NAE	0.37	0.37	0.39	0.39	0.42	0.42

From the results seen in table 2, we can notice that, the best 3D model was achieved at horizontal shift by 0.05% using KLT algorithm. Table 3, shows the comparison between the resulted 3D models using SIFT and KLT algorithms with image (3) using Performance Metrics (P.M).

Table 3: Comparison between the resulted 3D models according to 3D Reconstruction Using Horizontal Shift with image (3)

P.M	Shift by 0.05%		Shift by 0.1%		Shift by 0.2%	
	SIFT	KLT	SIFT	KLT	SIFT	KLT
MSE	3.75e+03	3.79e+03	3.94e+03	3.94e+03	4.14e+03	4.06e+03
PSNR	12.39	12.33	12.18	12.18	11.96	12.05
NAE	0.35	0.36	0.38	0.38	0.42	0.41

From the results seen in table 3, we can notice that, the best 3D model was achieved at horizontal shift by 0.05% using SIFT algorithm.

5.2 First Proposed Method

A rotation by four angles (30, 45, 60, and 90) was applied on the three test images according to the first method shown in fig. 2. Table 4, shows the comparison between the resulted 3D models using SIFT and KLT algorithms with image (1) using Performance Metrics (P.M).

Table 4: Comparison between the resulted 3D models according to the first proposed method with image (1)

P.M	Rotation by 30 deg.		Rotation by 45 deg.		Rotation by 60 deg.		Rotation by 90 deg.	
	SIFT	KLT	SIFT	KLT	SIFT	KLT	SIFT	KLT
MSE	9.08e+3	8.99e+3	9.69e+3	9.72e+3	9.41e+3	9.2e+3	4.64e+3	3.78e+3
PSNR	8.55	8.59	8.27	8.26	8.39	8.49	11.47	12.36
NAE	0.66	0.66	0.69	0.7	0.67	0.67	0.41	0.33

From the results seen in table 4, we can notice that, the best 3D model was achieved at rotation of image by 90 degree using KLT algorithm. Table 5, shows the comparison between the resulted 3D models using SIFT and KLT algorithms with image (2) using Performance Metrics (P.M).

Table 5: Comparison between the resulted 3D models according to the first proposed method with image (2)

P.M	Rotation by 30 deg.		Rotation by 45 deg.		Rotation by 60 deg.		Rotation by 90 deg.	
	SIFT	KLT	SIFT	KLT	SIFT	KLT	SIFT	KLT
MSE	8.65e+03	8.67e+03	9.44e+03	9.39e+03	8.66e+03	8.65e+03	4.39e+03	3.98e+03
PSNR	8.76	8.75	8.38	8.4	8.76	8.76	11.7	12.14
NAE	0.68	0.69	0.73	0.73	0.68	0.69	0.42	0.35

From the results seen in table 5, we can notice that, the best 3D model was achieved at rotation of image by 90 degree using KLT algorithm. Table 6, shows the comparison between the resulted 3D models using SIFT and KLT algorithms with image (3) using Performance Metrics (P.M).

Table 6: Comparison between the resulted 3D models according to the first proposed method with image (3)

P.M	Rotation by 30 deg.		Rotation by 45 deg.		Rotation by 60 deg.		Rotation by 90 deg.	
	SIFT	KLT	SIFT	KLT	SIFT	KLT	SIFT	KLT
MSE	8.81e+03	8.86e+03	9.68e+03	9.64e+03	9.13e+03	8.98e+03	4.21e+03	3.62e+03
PSNR	8.68	8.66	8.27	8.29	8.53	8.59	11.89	12.55
NAE	0.67	0.67	0.72	0.72	0.68	0.68	0.41	0.33

From the results seen in table 6, we can notice that, the best 3D model was achieved at rotation of image by 90 degree using KLT algorithm.

5.3 Results of the Second Proposed Method

Two 3D models were reconstructed using the original images according to the second method shown in fig. 3. Table 7, shows the comparison between the resulted 3D models using SIFT and KLT algorithms with image (1) using Performance Metrics (P.M).

Table 7: Comparison between the resulted 3D models according to the second proposed method with image (1)

P.M	Model (1)		Model (2)	
	SIFT	KLT	SIFT	KLT
MSE	4.28e+03	4.03e+03	4.13e+03	5.72e+03
PSNR	11.8	12.1	12	10.6
NAE	0.38	0.35	0.36	0.47

From the results seen in table 7, we can notice that, the best 3D model was model (1) using KLT algorithm. Table 8, shows the comparison between the resulted 3D models using SIFT and KLT algorithms with image (2) using Performance Metrics (P.M).

Table 8: Comparison between the resulted 3D models according to the second proposed method with image (2)

P.M	Model (1)		Model (2)	
	SIFT	KLT	SIFT	KLT
MSE	4.47e+03	4.26e+03	4.38e+03	6.1e+03
PSNR	11.6	11.8	11.7	10.3
NAE	0.4	0.38	0.39	0.51

From the results seen in table 8, we can notice that, the best 3D model was model (1) using KLT algorithm. Table 9, shows the comparison between the resulted 3D models using SIFT and KLT algorithms with image (3) using Performance Metrics (P.M).

Table 9: Comparison between the resulted 3D models according to the second proposed method with image (3)

P.M	Model (1)		Model (2)	
	SIFT	KLT	SIFT	KLT
MSE	3.87e+03	3.75e+03	5.4e+03	3.74e+03
PSNR	12.33	12.4	10.8	12.4
NAE	0.36	0.34	0.5	0.34

From the results seen in table 9, we can notice that, the best 3D model was model (2) using KLT algorithm.

5.4 Results of The third Proposed Method

Four 3D models were reconstructed using the original images according to the third proposed method shown in fig. 4. Table 10, shows the comparison between the resulted 3D models using SIFT and KLT algorithms with image (1) using Performance Metrics (P.M).

Table 10: Comparison between the resulted 3D models according to the third proposed method with image (1)

P.M	Model (1)		Model (2)		Model (3)		Model (4)	
	SIFT	KLT	SIFT	KLT	SIFT	KLT	SIFT	KLT
MSE	9.16e+3	8.99e+3	9.76e+3	9.72e+3	9.27e+3	9.27e+3	4.69e+3	4.71e+3
PSNR	8.51	8.59	8.23	8.25	8.46	8.46	11.42	11.4
NAE	0.66	0.66	0.7	0.7	0.68	0.67	0.41	0.42

From the results seen in table 10, we can notice that, the best 3D model was model (4) using KLT algorithm. Table 11, shows the comparison between the resulted 3D models using SIFT and KLT algorithms with image (2) using Performance Metrics (P.M).

Table 11: Comparison between the resulted 3D models according to the third proposed method with image (2)

P.M	Model (1)		Model (2)		Model (3)		Model (4)	
	SIFT	KLT	SIFT	KLT	SIFT	KLT	SIFT	KLT
MSE	8.65e+03	8.67e+03	9.37e+03	9.41e+03	8.62e+03	8.65e+03	4.43e+03	4.48e+03
PSNR	8.76	8.75	8.41	8.39	8.77	8.76	11.67	11.61
NAE	0.69	0.69	0.73	0.73	0.68	0.69	0.42	0.43

From the results seen in table 11, we can notice that, the best 3D model was model (4) using SIFT algorithm. Table 12, shows the comparison between the resulted 3D models using SIFT and KLT algorithms with image (3) using Performance Metrics (P.M).

Table 12: Comparison between the resulted 3D models according to the third proposed method with image (3)

P.M	Model (1)		Model (2)		Model (3)		Model (4)	
	SIFT	KLT	SIFT	KLT	SIFT	KLT	SIFT	KLT
MSE	8.87e+03	8.86e+03	9.6e+03	9.64e+03	9.02e+03	9.02e+03	4.25e+03	4.31e+03
PSNR	8.65	8.66	8.31	8.29	8.58	8.58	11.84	11.79
NAE	0.67	0.67	0.72	0.72	0.68	0.68	0.41	0.42

From the results seen in table 12, we can notice that, the best 3D model was model (4) using KLT algorithm.

5.5 Results of the Fourth proposed method

A vertical shift by (0.05, 0.1, and 0.2) % was applied on the three test images according to the fourth proposed method shown in fig. 5. Table 13, shows the comparison between the resulted 3D models using SIFT and KLT algorithms with image (1) using Performance Metrics (P.M).

Table 13: Comparison between the resulted 3D models according to the fourth proposed method with image (1)

P.M	Shift by 0.05%		Shift by 0.1%		Shift by 0.2%	
	SIFT	KLT	SIFT	KLT	SIFT	KLT
MSE	3.83e+03	3.94e+03	3.85e+03	3.99e+03	3.91e+03	4.02e+03
PSNR	12.3	12.18	12.28	12.12	12.21	12.09
NAE	0.33	0.34	0.34	0.34	0.35	0.36

From the results seen in table 13, we can notice that, the best 3D model was achieved at vertical shift by 0.05% using SIFT algorithm. Table 14, shows the comparison between the resulted 3D models using SIFT and KLT algorithms with image (2) using Performance Metrics (P.M).

Table 14: Comparison between the resulted 3D models according to the fourth proposed method with image (2)

P.M	Shift by 0.05%		Shift by 0.1%		Shift by 0.2%	
	SIFT	KLT	SIFT	KLT	SIFT	KLT
MSE	4.12e+03	4.19e+03	4.19e+03	4.25e+03	4.19e+03	4.19e+03
PSNR	11.98	11.89	11.91	11.85	11.91	11.91
NAE	0.37	0.37	0.37	0.38	0.38	0.38

From the results seen in table 14, we can notice that, the best 3D model was achieved at vertical shift by 0.05% using SIFT algorithm. Table 15, shows the comparison between the resulted 3D models using SIFT and KLT algorithms with image (3) using Performance Metrics (P.M).

Table 15: Comparison between the resulted 3D models according to the fourth proposed method with image (3)

P.M	Shift by 0.05%		Shift by 0.1%		Shift by 0.2%	
	SIFT	KLT	SIFT	KLT	SIFT	KLT
MSE	3.67e+03	3.73e+03	3.68e+03	3.75e+03	3.71e+03	3.74e+03
PSNR	12.48	12.42	12.48	12.39	12.44	12.39
NAE	0.34	0.34	0.33	0.34	0.34	0.35

From the results seen in table 15, we can notice that, the best 3D model was achieved at vertical shift by 0.05% using SIFT algorithm.

5.6 Results of the Fifth Proposed Method

A horizontal and vertical shift by (0.05, 0.1, and 0.2) % was applied on the three test images according to the fifth proposed method shown in fig. 6. Table 16, shows the comparison between the resulted 3D models using SIFT and KLT algorithms with image (1) using Performance Metrics (P.M).

Table 16: Comparison between the resulted 3D models according to the fifth proposed method with image (1)

P.M	Shift by 0.05%		Shift by 0.1%		Shift by 0.2%	
	SIFT	KLT	SIFT	KLT	SIFT	KLT
MSE	4.14e+03	4.14e+03	4.35e+03	4.39e+03	4.58e+03	4.72e+03
PSNR	11.97	11.96	11.75	11.71	11.52	11.39
NAE	0.36	0.36	0.38	0.39	0.42	0.43

From the results seen in table 16, we can notice that, the best 3D model was achieved at horizontal and vertical shift by 0.05% using SIFT algorithm. Table 17, shows the comparison between the resulted 3D models using SIFT and KLT algorithms with image (2) using Performance Metrics (P.M).

Table 17: Comparison between the resulted 3D models according to the fifth proposed method with image (2)

P.M	Shift by .05%		Shift by 0.1%		Shift by 0.2%	
	SIFT	KLT	SIFT	KLT	SIFT	KLT
MSE	4.23e+03	4.23e+03	4.28e+03	4.32e+03	4.44e+03	4.47e+03
PSNR	11.87	11.87	11.82	11.77	11.66	11.62
NAE	0.38	0.39	0.4	0.4	0.43	0.43

From the results seen in table 17, we can notice that, the best 3D model was achieved at horizontal and vertical shift by 0.05% using SIFT algorithm. Table 18, shows the comparison between the resulted 3D models using SIFT and KLT algorithms with image (3) using Performance Metrics (P.M).

Table 18: Comparison between the resulted 3D models according to the fifth proposed method with image (3)

P.M	Shift by 0.05%		Shift by 0.1%		Shift by 0.2%	
	SIFT	KLT	SIFT	KLT	SIFT	KLT
MSE	3.87e+03	3.82e+03	4.09e+03	4.01e+03	4.16e+03	4.18e+03
PSNR	12.25	12.31	12.01	12.06	11.94	11.92
NAE	0.36	0.36	0.39	0.38	0.42	0.42

From the results seen in table 18, we can notice that, the best 3D model was achieved at horizontal and vertical shift by 0.05% using KLT algorithm.

From all the previous results, we can notice that when using SIFT algorithm for feature extraction and matching, the more accurate 3D model with low value of (MSE and NAE) and high value of PSNR was achieved when a vertical shift by 0.05% was applied on the original images.

When using KLT algorithm for feature extraction and matching, the more accurate 3D model with low value of (MSE and NAE) and high value of PSNR was achieved when a rotation by 90 degree was applied on the original images. KLT gave better results than SIFT.

The time taken to produce a 3D model was about "45"seconds when using SIFT algorithm and about "19" seconds when using KLT algorithm. So, KLT has the advantage of small delay of time than SIFT.

6. Conclusion

In this paper, five methods have been presented for 3D object reconstruction using only one image. Due to poor information provided by a single image to reconstruct a 3D model, we tried to overcome this problem by creating a virtual image from the original image of an object to make the process of 3D reconstruction using two images instead of only one image. Kanade-Lucas-Tomasi (KLT) and Scale Invariant Feature Transform (SIFT) algorithms have been used for feature extraction and matching. Better performance have been gotten using KLT algorithm than using SIFT algorithm.

References

[1] S. Sengupta, Issues In 3D Reconstruction From Multiple Views, 2009.
[2] C. Wai, Y. Leung, and B.E. Hons, Efficient Methods For 3D Reconstruction From Multiple Images, 2006.

[3] P. Kovesi, "Shapelets Correlated With Surface Normals Produce Surfaces," 10th IEEE International Conference on Computer Vision, Beijing, pp: 994-1001, 2005.
[4] E. Delage, H. Lee, and A.Y. Ng, "A Dynamic Bayesian Network Model For Autonomous 3D Reconstruction From a Single Indoor Image," In Computer Vision and Pattern Recognition (CVPR), 2006.
[5] A. Torralba and A. Oliva, "Depth Estimation From Image Structure," IEEE Trans. Pattern Analysis and Machine Intelligence (PAMI), Vol. 24, No. 9, pp: 1–13, 2002.
[6] P. Felzenszwalb and D. Huttenlocher, "Efficient Graph-Based Image Segmentation," Int. Journal of Computer Vision Vol. 59,No. 2, pp: 167–181, 2004.
[7] Y. Chen and R. Cipolla, "Single and Sparse View 3D Reconstruction By Learning Shape Priors," Comput. Vis. Image Underst., Vol. 115, pp:586–602, 2011.
[12] J. T. Barron and J. Malik, "Color Constancy, Intrinsic Images, and Shape Estimation," In Europ. Conf. on Computer Vision, pp: 57–70, 2012.
[13] C. Hou, J. Yang, Z. Zhang, "Stereo Image Displaying Based On Both Physiological and Psychological Stereoscopy From Single Image," In international Journal of Imaging Systems and Technology – Multimedia, Vol. 18, Issue 2-3, pp: 146-149, 2008.
[14] K. Yoon, M. Shin, "Recognizing 3D Objects With 3D Information From Stereo Vision," International Conference on Pattern Recognition, pp: 4020-4023, 2010.
[15] V.S. Vora, A.C. Suthar, Y.N. Makwana, and S.J. Davda, "Analysis Of Compressed Image Quality Assessments," In International Journal of Advanced Engineering & Application, pp: 225-229, 2010.
[16] Lowe D., "Distinctive Image Features From Scale-Invariant Keypoints," International Journal of Computer Vision, Vol. 60, No. (2), pp: 91-110, 2004.
[17] L. Shyan, 3D Object Reconstruction Using Multiple-View Geometry: SIFT Detection, 2011.
[18] T. Shultz and L. A. Rodriguez, 3D Reconstruction From Two 2D Images, 2003.
[8] C. Colombo, A. D. Bimbo, A. Del, and F. Pernici, "Metric 3D Reconstruction and Texture Acquisition Of Surfaces Of Revolution From a Single Uncalibrated View," IEEE Transact. on Pattern Analysis and Machine Intelligence, Vol. 27, pp: 99–114, 2005.
[9] A. Criminisi, I. Reid, and A. Zisserman, "Single View Metrology," Int. J. Comput. Vision, Vol. 40, No. 2, pp: 123–148, 2000.
[10] M. Prasad, A. Zisserman, and A.W. Fitzgibbon, "Single View Reconstruction Of Curved Surfaces," In CVPR, pp: 1345–1354, 2006.
[11] E. Toeppe, M. R. Oswald, D. Cremers, and C. Rother. Imagebased 3D Modeling Via Cheeger Sets. In Asian Conference on Computer Vision (ACCV), pages 53–64, 2010.

Mohamed Abdel-Azim received the PhD degree in Electronics and Communications Engineering from the Faculty of Engineering-Mansoura University-Egypt by 2006. After that he worked as an assistant professor at the electronics & communications engineering department until now. He has 60 publications in various international journals and conferences. His current research interests are in multimedia processing, wireless communication systems, and field programmable gate array (FPGA) applications.

Essam Abdel-Latef received the B.Sc. in Electronics and Communications Engineering from the Faculty of Engineering-Zagazig University-Egypt by 2009. Currently he is pursuing his Master Degree in Mansoura University-Egypt. He worked as a demonstrator at the electronics & communications engineering department until now.

(a) (b) (c)

Fig. 7: Three test images of an object: (a) → Image (1), (b) → Image (2), and (c) → Image (3)

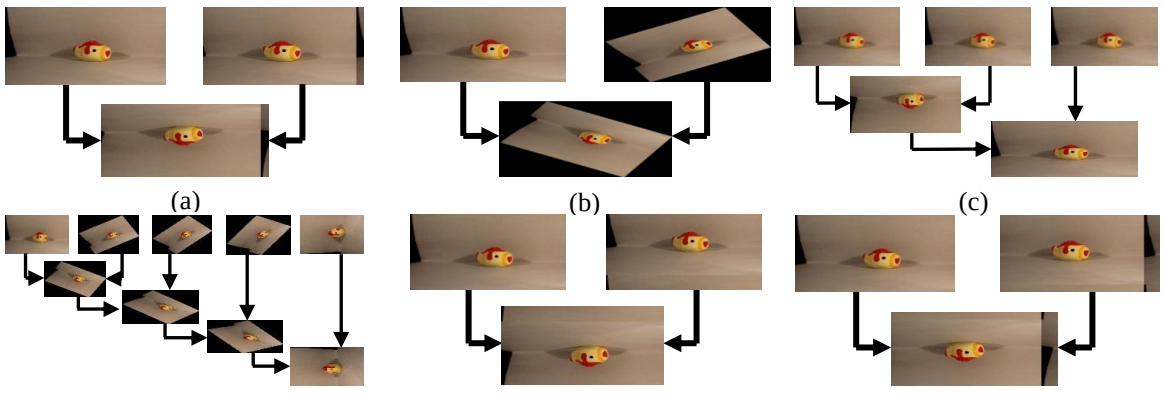

(a) (b) (c)

(d) (e) (f)

Fig. 8: Some results of 3D models reconstructed from image (1) : (a) → 3D Reconstruction Using Horizontal Shift, (b) → First Proposed Method, (c) → Second Proposed Method, (d) → Third Proposed Method,(e) → Fourth Proposed Method, and (f) → Fifth Proposed Method.

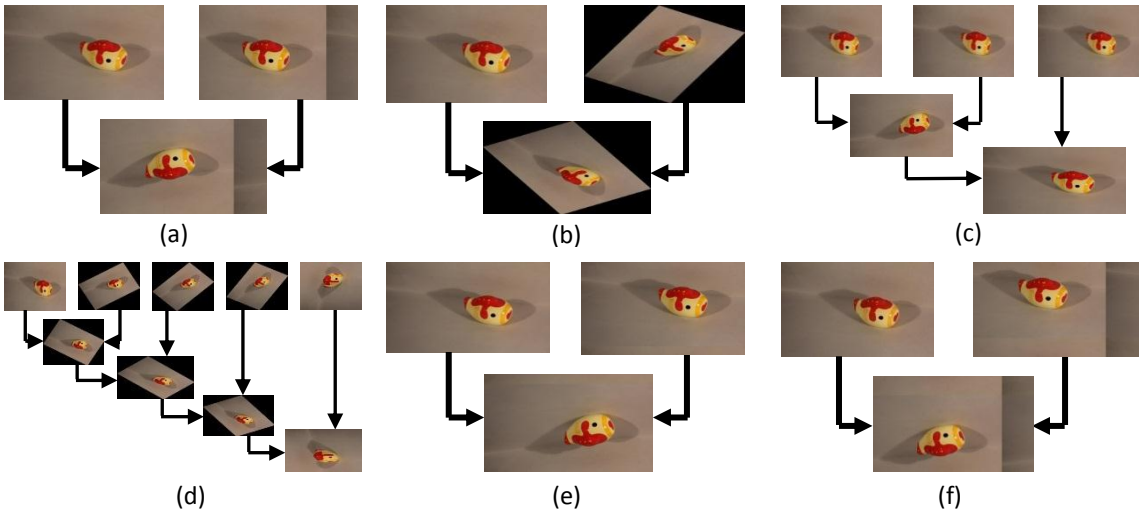

Fig. 9: Some results of 3D models reconstructed from image (2) : (a) → 3D Reconstruction Using Horizontal Shift, (b) → First Proposed Method, (c) → Second Proposed Method, (d) → Third Proposed Method, (e) → Fourth Proposed Method, and (f) → Fifth Proposed Method.

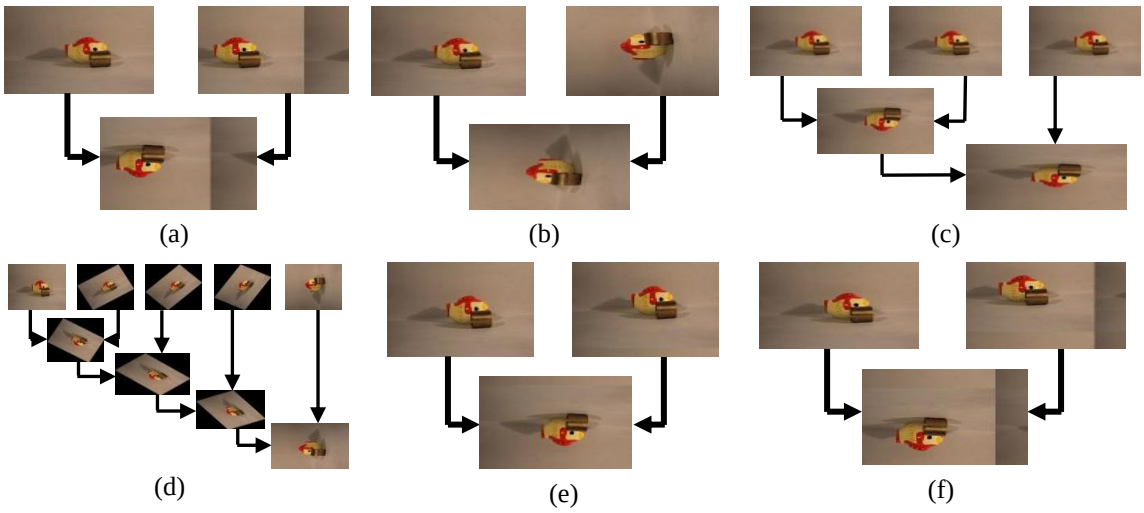

Fig. 10: Some results of 3D models reconstructed from image (3): (a) → 3D Reconstruction Using Horizontal Shift, (b) → First Proposed Method, (c) → Second Proposed Method, (d) → Third Proposed Method, (e) → Fourth Proposed Method, and (f) → Fifth Proposed Method.